Table II. Values of Parameters of Equation 1 for Various Mixtures at 303.15 and 313.15K

System	Temp, K	G_0	G_1	G_2	$\sigma(p)$, torr
Pyridine(1)–bromoform(2)	303.15	−0.5303	−0.2622	−0.1739	0.09
	313.15	−0.7037	0.1580	−0.0610	0.36
Pyridine(1)–chloroform(2)	303.15	−1.0799	0.3478	−0.2092	1.44
	313.15	−0.6219	0.0668	−0.0954	0.72
n-Hexane(1)–bromoform(2)	303.15	1.2122	0.3478	0.0901	2.02
	313.15	1.4436	−0.0273	0.3985	3.20
n-Hexane(1)–chloroform(2)	303.15	0.6077	0.0013	−0.2391	0.57
	313.15	0.6585	−0.1418	−0.1226	0.79
Benzene(1)–bromoform(2)	303.15	0.1653	0.0969	0.0440	0.19
	313.15	0.1102	0.0605	0.0348	0.12

Literature Cited

(1) Adya, A. K., Mahl, B. S., Singh, P. P., *J. Chem. Thermodyn.*, **5**, 393 (1973).
(2) Barker, J. A., *Aust. J. Chem.*, **6**, 207 (1953).
(3) Fenby, D. V., *ibid.*, **26**, 1143 (1973).
(4) Reid, R. C., Sherwood, T. K., "The Properties of Gases and Liquids," McGraw-Hill, New York, N.Y., 1958.
(5) Scatchard, G., Ticknor, L. B., *J. Am. Chem. Soc.*, **74**, 3724 (1952).
(6) Sharma, B. R., Singh, P. P., *J. Chem. Thermodyn.*, **5**, 361 (1973).
(7) Taha, A. A., Grigsby, R. D., Johnson, J. R., Christian, S. D., Affsprung, H. E., *J. Chem. Educ.*, **43**, 432 (1966).
(8) Timmerman, J., "Physico-chemical Constants of Pure Organic Compounds," Elsevier, Amsterdam, The Netherlands, 1950.
(9) Vogel, A., "Practical Organic Chemistry," Longmans, Green, London, England, 1968.

Received for review July 15, 1974. Accepted April 19, 1975.

Low-Temperature *K* Data for Methane–*n*-Pentane

LeRoy C. Kahre
Research and Development, Phillips Petroleum Co., Bartlesville, Okla. 74004

Phase equilibrium data are presented for the methane–*n*-pentane system at low temperatures and high pressures. Seven isotherms from 50° to −140°F and 50 to 2300 psia are obtained. A region of triple-valued dew points is observed for each of the isotherms near or below the methane critical temperature. Measured critical conditions are in good agreement with previously reported values.

The current interest in the recovery of light hydrocarbons from natural gas necessitates the obtaining of fundamental vapor-liquid equilibrium data for at least the binary systems. Data for the methane–*n*-butane system were reported previously (*4*), and this work is merely an extension to another system where literature data are not available.

Experimental

The experimental equipment (Figure 1) is the same as that used for the previous work (*4*). It consists of a vapor recirculating equilibrium cell immersed in a suitable liquid bath, a gas-liquid chromatography unit for analyses of both vapor and liquid samples, and associated temperature and pressure measuring instruments. For most of the work the samples were analyzed with the use of a component peak height (compared to a pure component at the same partial pressure) as the measure of concentration. However, near the end of the program, the output from the thermal conductivity detector was tied to a central computer so that peak areas could also be measured. No significant difference was found between the two methods of calculation. Table I presents a comparison between the pentane concentration of samples gravimetrically synthesized and that analyzed by the peak

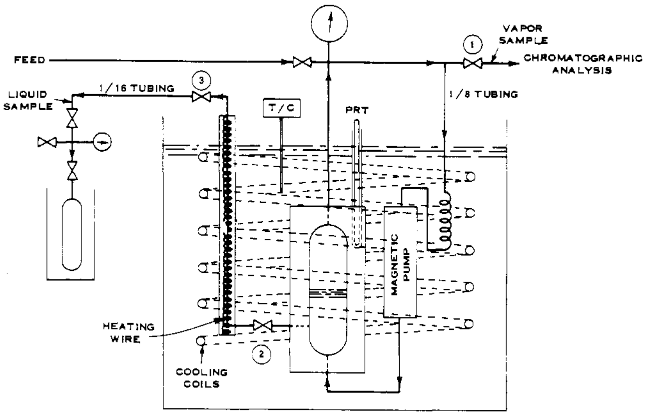

Figure 1. Schematic diagram of experimental equipment

Table I. Analyses of Synthetic Samples of Methane–*n*-Pentane

n-Pentane concn, mol %		
Synthesized	Analyzed	% Dev
86.08	85.52	0.65
51.00	50.82	0.35
28.41	28.41	0.0
13.82	13.53	2.1
0.934	0.904	3.2
0.110	0.111	0.9
0.0130[a]	0.0124	4.6

[a] Synthesized by diluting previous sample.

Table II. Phase Equilibrium Data for Methane–*n*-Pentane

Pressure		Composition, mole fraction methane		Pentane partial press, psia	*K*-value	
Psia	Atm	Vapor	Liquid		Methane	Pentane
		T = 50.0°F = 10.0°C				
5.51	0.375[a]	0.00	0.00	5.5	...	1.00
100	6.80	0.9376	0.036[b]	6.2	26.0	0.0647
200	13.61	0.9650	0.075[b]	7.0	12.9	0.0378
300	20.41	0.9735	0.113	7.95	8.62	0.0299
900	61.24	0.9810	0.320	17.1	3.07	0.0279
1300	88.45	0.9751	0.438	32.4	2.23	0.0443
1700	115.67	0.9637	0.558	61.7	1.73	0.0821
2000	136.08	0.9436	0.649	113	1.45	0.161
2200	149.67	0.9306	0.725	153	1.28	0.252
2300	156.49	Critical opalescence observed				
		T = 0.0°F = −17.8°C				
1.46	0.099	0.00	0.00	1.46	...	1.00
50	3.40	0.9686	0.023[b]	1.57	42.1	0.0321
100	6.80	0.9832	0.046[b]	1.68	21.4	0.0176
200	13.61	0.9902	0.095	1.96	10.4	0.0108
400	27.22	0.9932	0.183	2.73	5.43	0.0083
600	40.82	0.9935	0.267	3.90	3.72	0.0089
800	54.43	0.9924	0.348	6.08	2.85	0.0117
1000	68.04	0.9909	0.424	9.10	2.34	0.0158
1500	102.06	0.9807	0.597	29.0	1.64	0.0479
1800	122.47	0.9690	0.712	55.8	1.36	0.108
2000	136.08	0.9449	0.811	110	1.165	0.291
2011	136.83	Critical opalescence observed				
		T = −50.0°F = −45.6°C				
0.26	0.018	0.00	0.00	0.26	...	1.00
50	3.40	0.9938	0.031[b]	0.31	32.1	0.0064
100	6.80	0.9966	0.062[b]	0.34	16.1	0.0036
400	27.22	0.9983	0.248	0.68	4.03	0.0023
700	47.63	0.9976	0.411	1.68	2.43	0.0041
1000	68.04	0.9951	0.564	4.9	1.76	0.0112
1200	81.65	0.9906	0.657	11.3	1.51	0.0274
1400	95.26	0.9833	0.770	23.4	1.28	0.0726
1480	100.70	0.9702	0.831	44.1	1.17	0.176
1508	102.60	Critical opalescence observed				
		T = −103.0°F = −75.0°C				
0.020	0.0014	0.00	0.00	0.020	...	1.00
50	3.40	0.99950	0.051[b]	0.025	19.6	0.00053
100	6.80	0.99971	0.1015	0.029	9.85	0.00032
200	13.61	0.99978	0.205	0.044	4.87	0.00028
300	20.41	0.99978	0.298[b]	0.066	3.35	0.00031
400	27.22	0.99976	0.391	0.096	2.56	0.00039
500	34.02	0.99967	0.485[b]	0.165	2.06	0.00064
600	40.82	0.99947	0.595	0.318	1.68	0.00131
700	47.63	0.99890	0.737	0.77	1.355	0.00418
750	51.03	0.9980	0.866	1.50	1.15	0.015
770	52.39	0.9970	0.956	2.31	1.04	0.068
787	53.55	Critical opalescence observed				
		T = −116.0°F = −82.2°C				
0.095	0.00065	0.00	0.00	0.0095	...	1.00
50	3.40	0.99976	0.058[b]	0.012	17.2	0.000255
100	6.80	0.99984	0.116	0.016	8.62	0.00018
200	13.61	0.99988	0.228	0.024	4.39	0.000155
300	20.41	0.99988	0.343[b]	0.036	2.92	0.00018
400	27.22	0.99984	0.465	0.064	2.15	0.00030
500	34.02	0.99976	0.609[b]	0.120	1.64	0.00061
600	40.82	0.99946	0.817	0.324	1.22	0.00295
624	42.46	0.99928	0.9311	0.449	1.07	0.01045
642	43.68	0.99922	0.9732	0.500	1.027	0.0291
651	44.29	0.99923	...	0.501	...	...
661	44.97	0.99931	...	0.456	...	...
674	45.86	Critical opalescence observed				

Table II. Continued

Pressure		Composition, mole fraction methane		Pentane partial press, psia	K-value	
Psia	Atm	Vapor	Liquid		Methane	Pentane
		$T = -125.0°F = -87.2°C$				
0.0056	0.00038	0.00	0.00	0.0056[a]	. . .	1.00
50	3.40	0.99983	0.064[b]	0.0085	15.6	0.000182
100	6.80	0.999903	0.128	0.0097	7.81	0.000111
200	13.61	0.999921	0.260	0.0158	3.85	0.000107
300	20.41	0.999917	0.392	0.0249	2.55	0.000137
400	27.22	0.999885	0.540	0.0460	1.85	0.000250
450	30.62	0.99986	0.618	0.063	1.62	0.00037
500	34.02	0.99979	0.740	0.105	1.35	0.00081
530	36.06	0.99973	0.865	0.143	1.16	0.0020
544	37.01	0.99971	0.9545	0.158	1.047	0.0064
559	38.03	0.99978	0.9715	0.123	1.029	0.0077
578	39.33	1.00	1.00	. . .	1.00	. . .
		$T = -140.0°F = -95.6°C$				
0.0022	0.00015	0.00	0.00	0.0022	. . .	1.00
50	3.40	0.999937	0.0785[b]	0.00315	12.7	0.000068
100	6.80	0.999961	0.157	0.0039	6.37	0.000046
200	13.61	0.999970	0.321	0.0060	3.12	0.000044
300	20.41	0.999956	0.510	0.0132	1.96	0.000090
350	23.81	0.999949	0.623	0.0178	1.605	0.000135
398	27.08	0.999938	0.829	0.025	1.21	0.00036
410	27.90	0.999935	0.897	0.027	1.11	0.00063
441	30.01	1.00	1.00	. . .	1.00	. . .

[a] *n*-Pentane vapor pressures from Carruth and Kobayashi (*1*). [b] Estimated value.

height method. The greatest deviation was 4.6% at a pentane concentration of 130 ppm.

Details of the experimental procedure can be found in the previous publication. Phillips research grade methane (99.98%) and *n*-pentane (99.99%) were used.

Results

Experimental data are tabulated in Table II. The concentrations of methane in the liquid phase at low pressures (noted in Table II) were calculated by assuming a linear relationship between concentration and methane partial pressure (Henry's law). Certain other liquid-phase compositions (also noted in Table II) were estimated by interpolation. It should be recognized that the tabulated concentration of methane in the 0.999+ range is actually 1.0 minus the concentration of *n*-pentane. The Phillips research grade methane (99.98%) used in this work is not as pure as some of the concentrations listed since it contains minor amounts (0.01%) of nitrogen and ethane.

Pressure-composition relationships are shown in Figure 2 for the seven isotherms obtained. Most of the vapor compositions are omitted since they are nearly pure methane. The vapor compositions for the four lower isotherms are shown on an expanded scale in Figure 3. The three lowest isotherms of this figure all show an unusual S-shaped pressure-composition curve. At constant composition there are therefore three equilibrium dew point pressures. This phenomenon was observed previously for the methane-butane system and for this system by Chen et al. (*2*). A comparison with the data of Chen et al. for the −103°F isotherm is also shown in this figure. The deviation between the two sets of data appears large on this plot and, in fact, based on the pentane concentration, it is 20–30%. However, considering the level of pentane concentration (200–500 ppm), this deviation between two laboratories does not appear unreasonable. This is the only isotherm in common for the two sets of data.

Figure 4 presents the effect of pressure on the pentane partial pressure. As discussed previously (*4*), this enhancement relationship is quite valuable in the evaluation of vapor-phase compositions since the curves should extrapolate to the pure component vapor pressure.

Figure 5 presents the data in the form of *K* values vs. pressure, and Figure 6 shows the critical pressure-temperature relationship for this system. The critical locus appears to agree quite well with previous data.

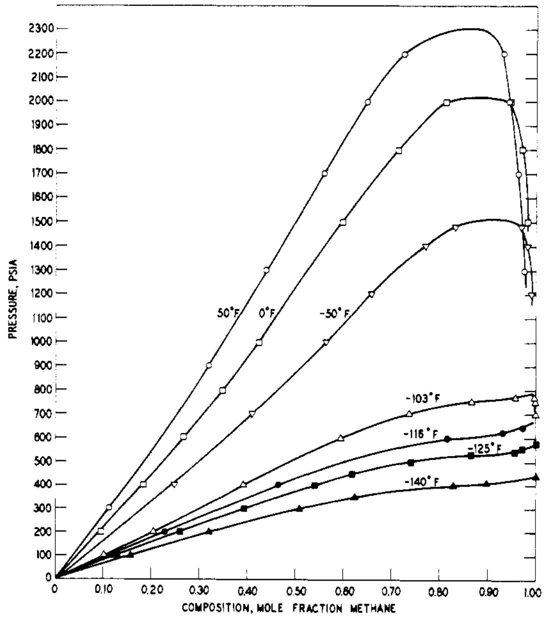

Figure 2. Isothermal pressure-composition diagrams for methane-*n*-pentane

Figures 7 and 8 compare the solubilities of methane in pentane with that in butane and propane near or below the methane critical temperature. Figure 7 also shows the excellent agreement between the two sets of methane–butane data at −140°F. At low temperatures the methane–pentane curves have a more distinct point of inflection than the lighter hydrocarbons. This observation is reasonable since the tendency toward two liquid phases (a horizontal *P-X* curve) should increase with increasing carbon number in the homologous series.

Discussion of Errors

The temperature was controlled and measured with a resistance thermometer to ±0.005°F but was allowed to vary nearly ±0.1°F between points on the same isotherm for the sake of efficiency. The pressures, with the exception of those above 2000 psia, are believed to be accurate to ±2 psia since they were measured with a calibrated 2000-psia Heise gauge. Those above 2000 psia (50°F isotherm) were measured with a 5000-psia Heise gauge and therefore are less accurate.

The primary source of error is in obtaining the right samples and analyzing them. The methane was always present in appreciable quantities; thus, its concentration is believed to be accurate to ±2%. The precision of the determination of pentane concentration (based on replicate samples) was normally within ±5% of the amount present. A comparison with synthetic samples (Table I) indicates that the accuracy should

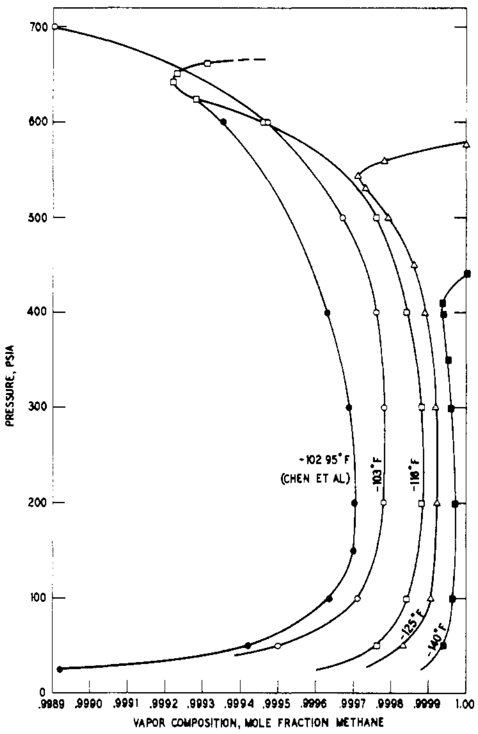

Figure 3. Pressure-vapor composition for methane–*n*-pentane (expanded scale)

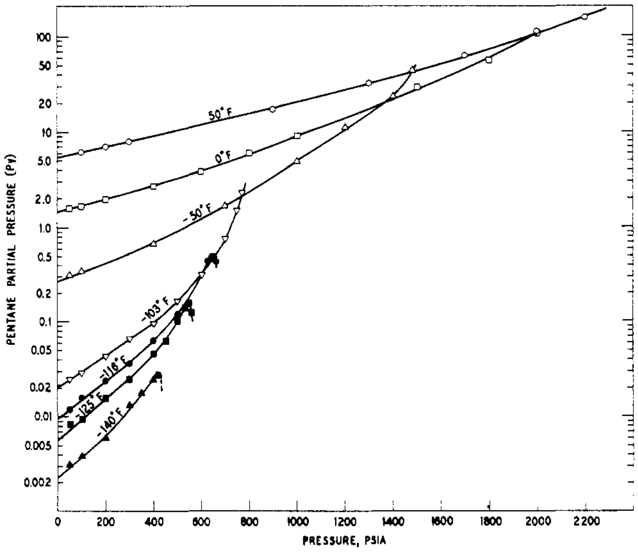

Figure 4. Enhancement of vapor phase with *n*-pentane

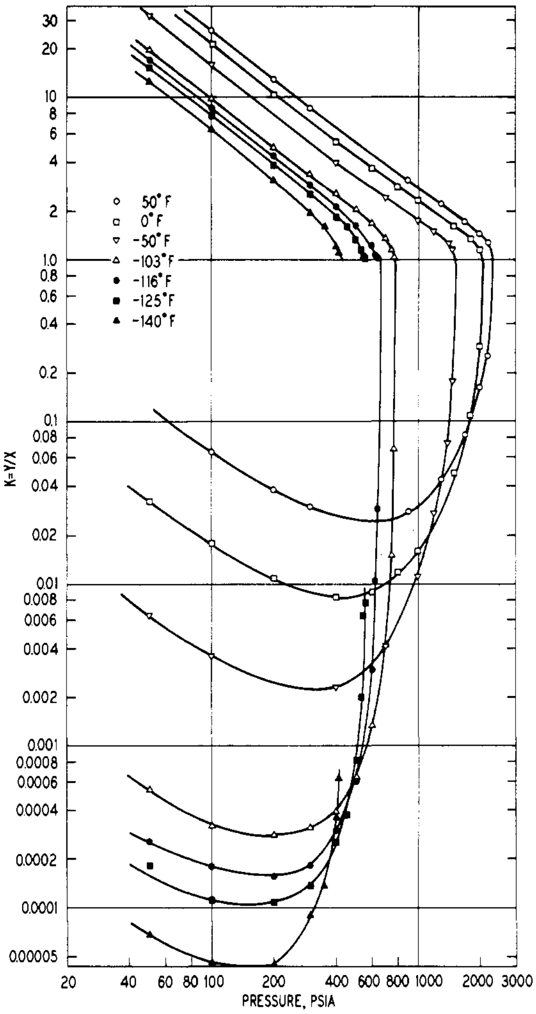

Figure 5. Isothermal *K* values for methane–*n*-pentane

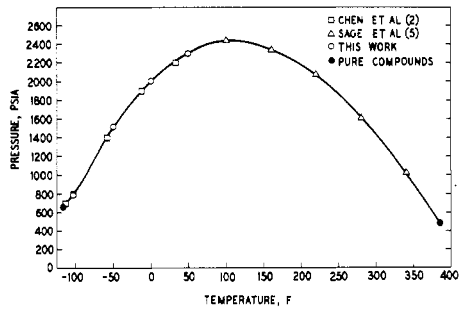

Figure 6. Critical locus for methane–*n*-pentane

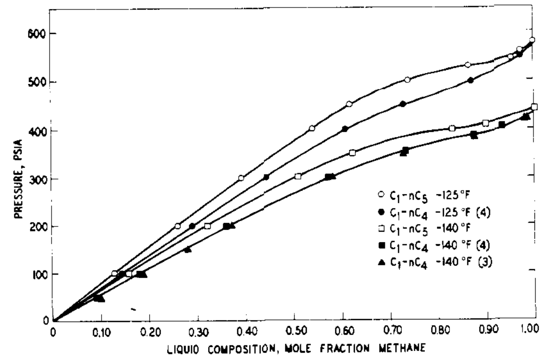

Figure 7. Comparison of methane–pentane and methane–butane at low temperatures

also be in this range. At low pentane concentrations (less than 0.1% in the vapor or less than 10% in the liquid), however, deviations between duplicate samples were sometimes ±10% of the pentane present.

Based on these considerations, a somewhat subjective estimate of error in the K value is ±2% for methane, ±5% for pentane to −50°F, and ±10% for pentane at temperatures below −50°F.

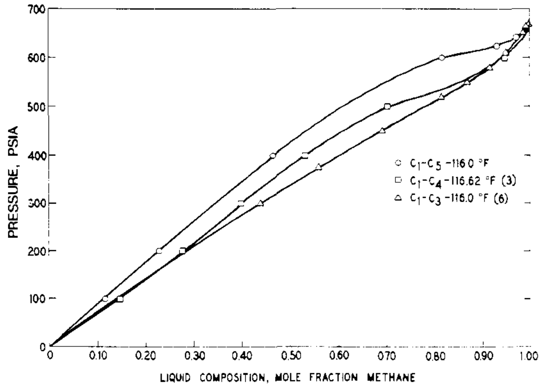

Figure 8. Solubility of methane in propane, butane, and pentane near methane critical temperature

Literature Cited

(1) Carruth, G. F., Kobayashi, R., *J. Chem. Eng. Data,* **18** (2), 115 (1973).
(2) Chen, R.J.J., Chappelear, P. S., Kobayashi, R., *ibid.,* **19** (1), 58 (1974).
(3) Elliott, D. G., Chen, R.J.J., Chappelear, P. S., Kobayashi, R., *ibid.,* p 71.
(4) Kahre, L. C., *ibid.,* p 67.
(5) Sage, B. H., Reamer, H. H., Olds, R. H., Lacey, W. N., *Ind. Eng. Chem.,* **34,** 1108 (1942).
(6) Wichterle, I., Kobayashi, R., *J. Chem. Eng. Data,* **17** (1), 4 (1972).

Received for review September 6, 1974. Accepted May 27, 1975.

Vapor-Liquid Equilibria of Acetone, Isopropenyl Acetate, and Acetic Anhydride

Michael F. Kozempel[1] **and C. Michael Kelly**[2]
U.S. Department of Agriculture, Agricultural Research Service, Eastern Regional Research Center, Philadelphia, Pa. 19118

Isothermal vapor-liquid equilibria of acetone–isopropenyl acetate–acetic anhydride at 55 °C were studied. The data were obtained with a commercially available Othmer still and can be satisfactorily correlated with Raoult's law for distillation calculations.

Work is in progress in this laboratory to develop a commercially feasible process for the production of isopropenyl stearate. One potential process is based on the ester interchange reaction of stearic acid with isopropenyl acetate (IPA) to form isopropenyl stearate. The reactor product contains the volatiles, acetone, IPA, and acetic anhydride (AC_2O). It was the purpose of this study to determine the vapor-liquid equilibria (VLE) of the ternary system acetone–IPA–AC_2O for use in the design of distillation columns for separating these compounds from the nonvolatile products and purifying the volatiles for recycle.

Experimental

Materials. Acetone and AC_2O were ACS reagent grade chemicals purchased from J. T. Baker Chemical Co. IPA was purchased from Matheson Coleman & Bell. Acetone, IPA, and AC_2O were purified by distillation as described under the Apparatus and procedure section. Gas-liquid chromatography analysis of ternary samples indicated maximum impurities of 0.5 wt %.

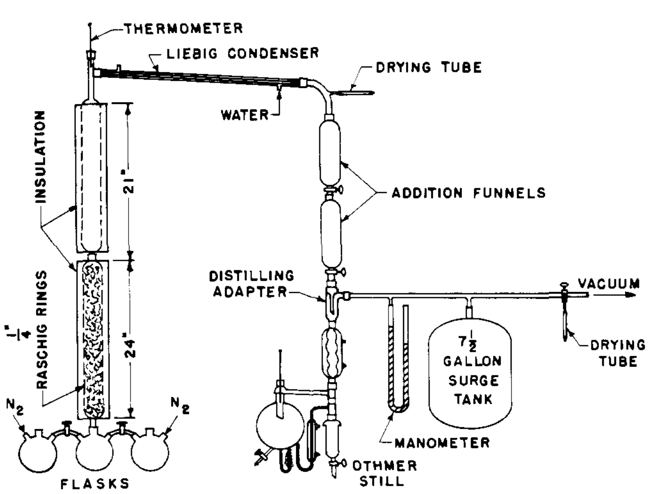

Figure 1. Experimental apparatus

---

[1] To whom correspondence should be addressed.
[2] Present address, Villanova University, Villanova, Pa. 19085.